10th International Conference on Fracture Mechanics of Concrete and Concrete Structures
FraMCoS-X
G. Pijaudier-Cabot, P. Grassl and C. La Borderie (Eds)
https://doi.org/10.21012/FC10.235657

NUMERICAL SIMULATION OF MICROCRACKING INDUCED BY DRYING SHRINKAGE IN EARLY AGE CEMENT PASTES

ABDERRAHMANE RHARDANE, FREDERIC GRONDIN AND SYED YASIR ALAM

Institut de Recherche en Génie Civil et Mécanique, GeM-UMR 6183, Centrale Nantes – Université de Nantes – CNRS, 1 rue de la Noë, 44321 Nantes, FRANCE
e-mail: {abderrahmane.rhardane; frederic.grondin; syed-yasir.alam}@ec-nantes.fr, www.ec-nantes.fr

Key words: Damage, Cement paste, Drying shrinkage, Early age, Microcracking

Abstract: A modelling approach is proposed to simulate drying shrinkage and shrinkage-induced microcracking in cement paste. The proposed approach takes into consideration the heterogeneous nature of the cement paste as well as the development of the microstructure due to fast-paced hydration at early-ages. Simulations show that the development of microcracking depends on the initial conditions, the drying depth and the drying threshold age.

1 INTRODUCTION

When cementitious materials are exposed to the ambient atmosphere without further curing, the gradient of humidity triggers the loss of moisture which evaporates from the capillary porosity of cement paste. Furthermore, in the absence of curing, the internal water content decreases due to self-desiccation. These two phenomena contribute to the total shrinkage of the material, and the pressure build-up in the pore network may lead to the development of microcracks in the cement matrix in the case of severe drying. The evaluation and the prediction of drying-induced microcracking is therefore of great importance.

The mechanisms of autogenous and drying shrinkages in early-age cement paste are only fairly understood [1]–[4] and some models have been proposed to predict crack initiation due to drying in cement-based materials [5]. However, the assessment of microcracking in cement pastes using experimental testing is generally difficult [6]. Numerical modelling offers another perspective to investigate the role of drying on the initiation of microcracks. Most numerical studies already proposed to simulate drying shrinkage are limited to the mesoscale (mortar and concrete) [7]–[10]. The assessment of microcracking is therefore only inferred given that the heterogeneity of the binding cement paste microstructure is not explicitly represented. In fact, it is more compelling to start the investigation from the scale of cement paste where the mechanisms of drying shrinkage take place. Microscale simulation of drying in cementitious materials is a recent topic of interest, thanks to the development of powerful numerical tools to simulate the complex microstructure of cement paste. In [11], shrinkage was simulated at the microscale using a virtual microstructure of cement paste generated by the hydration model HYMOSTRUC3D [12]. The heterogeneous microstructure is converted into a lattice network and the pore pressure induced by drying is directly affected to the pore surfaces. However, since the microstructure is fixed, the approach followed by the authors is limited to well-hydrated cement pastes, and cannot be used at early ages when the microstructure

changes considerably. In addition to that, the fracture of cement phases was not taken into account.

The proposed modelling approach attempts to address the deficiencies of the previously proposed approaches. In this article, drying is simulated using a FE micromechanical model which takes into account the heterogeneous nature of the cement paste and its evolving microstructure at early ages. Shrinkage due to drying and self-desiccation were calculated and directly incorporated on the pore walls. The novelty of this method is that the FE mesh of the cement paste is continuously updated at each step of the computations without the need for any calibrated coefficients or empirical equations that describe the evolution of the cement paste properties, such as stiffness, strength and pore size distribution. Also, a constitutive damage law is given to cement phases, which makes it possible to simulate damage due to local stresses in the paste.

2 BASICS OF THE MODELLING APPROACH

Simulations of dying are conducted on 2D representative elementary volumes (REVs) of cement paste with a unit size of 100µm. To illustrate the effect of the severity of drying, the REV is assumed to represent different layers of a cement paste beam with height L at depth d. The relative humidity is taken to be initially homogeneous (RH_0) inside the beam which undergoes unidirectional drying. The top surface is exposed to the ambient humidity (RH_∞) and the bottom surface is isolated, as illustrated in Figure 1.

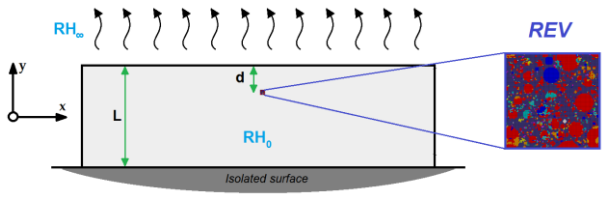

Figure 1: Illustration of an REV inside a cement paste beam subjected to 1D-drying.

2.1 Simulation of the cement hydration

The first step of the simulation is the generation of the cement microstructure. Many cement hydration models are proposed in the literature (HYMOSTRU3D, CEMHYD3D, HydratiCA, µic, etc.). Here, the hydration modelling platform VCCTL [13] is used. Its voxelized architecture as well as the explicit representation of the cement phases makes it easier to incorporate distinct behaviour to different parts of the mesh. To construct the virtual microstructure, the cement properties (mineral composition of clinker, amount of gypsum, activation energy and particle size distribution), the water-to-cement ratio, the temperature and the isothermal calorimetry curve of the cement paste are fed as input to the model. The code uses the principles of cellular automata to mimic the dissolution-precipitation steps of cement hydration. Since hydration proceeds by cycles, the calorimetry curve is used to identify the correct age of the cement paste at each cycle.

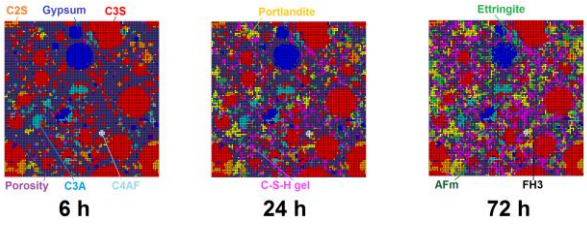

Figure 2: Simulation of the hydration of cement paste using VCCTL.

2.2 Implementation of the evolving cement paste in early-age simulations

In order to take into account the evolving nature of the microstructure, a first simulation of the cement hydration is conducted in order to determine the evolution of the degree of hydration for the first 72 hours. The degree of hydration is subdivided into 150 computation steps and the corresponding ages are calculated. This method of discretizing the degree of hydration and not the time scale is done to ensure that the cement paste evolves at a constant rate between two consecutive time steps. The initial microstructure of cement paste (unhydrated cement particles + initial water content) is first generated and converted into a mesh using the finite element code Cast3M [14]. At each step i of the simulation,

the mesh is first updated by reading the new microstructure that corresponds to the age t_i from the hydration model, as shown in the simulation algorithm presented in Figure 3.

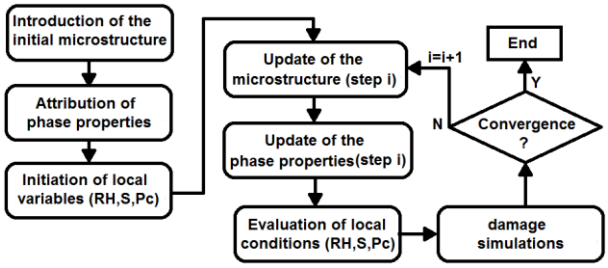

Figure 3: Simulation approach of drying in a hydrating microstructure of cement paste.

2.2 Constitutive behaviour of the cement paste phases

The constitutive law used in this study is the damage law developed by Fichant et al. [15], [16], which is extensively used for the modelling of cementitious materials. For the sake of simplicity, the same damage behaviour was attributed to all cement phases. However, different phases have distinct properties. The model takes into account the dissymmetry between tension and compression:

$$\boldsymbol{\sigma} = (1\text{-}D_T)\{\mathbb{C}^0\boldsymbol{\varepsilon}\}_+ + (1\text{-}D_C)\{\mathbb{C}^0\boldsymbol{\varepsilon}\}_- \qquad (1)$$

where D_T and D_C are the damage variables and $\{\bullet\}$ are the Macaulay brackets. In the case of cement phases, it is assumed that damage grows primarily via tension. The expression of the evolution law takes the following form:

$$D_T = 1 - \frac{\kappa_0}{\varepsilon_{eq}} \exp\left[-B_T\left(\varepsilon_{eq} - \kappa_0\right)\right] \qquad (2)$$

with ε_{eq} the Mazars equivalent strain:

$$\varepsilon_{eq} = \sqrt{\sum \{\varepsilon_{ii}\}_+^2} \qquad (3)$$

The model parameters κ_0 and B_T can be linked to the physical properties of cement phases (Young's modulus E, tensile strength f_t, and fracture energy G_f):

$$\kappa_0 = \frac{f_t}{E}, \qquad B_T = \frac{f_t}{\frac{G_f}{h} - \frac{f_t^2}{2E}} \qquad (4)$$

with h being the finite element size (1µm).

The properties used in this study were compiled from the literature of mineral cement phases and validated against experimental tests of compression and three-point bending of cement paste. Table 1 lists the properties of the main cement phases. A complete list of the mechanical properties of all the phases can be found in [17]. These properties are considered intrinsic to the cement phases and do not change with the composition or the degree of hydration. It is rather the evolving volume distributions of these phases that change the properties of the macroscopic material.

As shown in Figure 3, the properties of each voxel in the microstructure mesh need to be updated at each step, according the newly formed cement phase.

Table 1: Properties of the main cement paste phases.

Phase	E (GPa)	ν (-)	f_t (MPa)	G_f (J/m²)
C_3S	137.4	0.30	430.7	65.8
C_2S	135.5	0.30	396.0	56.3
C_3A	145.2	0.28	534.6	94.3
C_4AF	150.8	0.32	470.3	72.5
Gypsum	44.5	0.33	29.6	0.98
CH	43.5	0.29	73.8	6.1
C-S-H	23.8	0.24	55.0	5.9
Ettringite	24.1	0.32	39.6	3.2
AFm	43.2	0.29	262.4	77.3

2.3 Modelling of the moisture content in cement paste

The evolution of local conditions (relative humidity, saturation degree, pore pressure) is tracked throughout the simulations using internal variables which are re-evaluated at every computation step (cf. Figure 3). The governing equation for the variation of local relative humidity is Fick's diffusion law:

$$\frac{\partial RH}{\partial t} = D\frac{\partial^2 RH}{\partial y^2} \qquad (5)$$

where RH depends on the drying depth, and diffusivity coefficient D follows the non-linear model given by [18]:

$$D = D_0\left(\alpha_0 + \frac{1-\alpha_0}{1+\left(\frac{1-RH}{1-RH_c}\right)^n}\right) \quad (6)$$

With D_0=1.67×10^{-10}m²/s, α_0=5%, n=16 and RH_c=75% for cement paste [18].

Since the REV is small relative to the beam size (100×100µm), it is assumed that the local humidity inside the REV is homogeneous. However, the evolution of the local humidity depends on the drying depth, as illustrated in Figure 1. The approximation solution to Eq. 5 is given as [19]:

$$RH(t) = RH_0 + (RH_\infty - RH_0) \times \left[erfc\left(-\frac{d}{2\sqrt{Dt}}\right) + erfc\left(\frac{2L+d}{2\sqrt{Dt}}\right)\right] \quad (7)$$

The equation above can be modified to introduce a delay in the initiation of drying by replacing the time t with $t - t_0$ where t_0 is the drying threshold age.

2.4 Expression of equivalent pore pressure

The desorption curve of the cement paste depends on the pore network which varies with the paste composition and the degree of hydration [20]. Different models are proposed for the prediction of the desorption isotherms [21]. In this study, the three-parameter BSB model [22] is used. The water content can be expressed as a function of the relative humidity (RH≥5%):

$$W = \frac{CkV_mRH}{(1-kRH)[1+(C-1)kRH]} \quad (8)$$

Where V_m, k and C are model parameters that depend on the age of the cement paste, the w/c ratio, the cement type and the temperature (cf. [21]). Therefore, this equation takes into account the evolution of the pore network with the hydration time. Using this equation, the saturation degree can be expressed in terms of the relative humidity:

$$S(RH) = \frac{W(RH)}{W(RH_0)} \quad (9)$$

By neglecting the effect of dissolved ions in the pore solution, the capillary pressure can be calculated using:

$$p_C(t) = \frac{RT}{v_m}\ln RH(t) \quad (10)$$

With R=8.314J/mol/K, T=293.15K (20°C) and v_m=18.015cm^3/mol. The additional pressure induced by the pore interfaces is calculated according to [19], [23]:

$$U(S) = \int_S^1 p_C(S')dS' \quad (11)$$

Finally, the equivalent pore pressure applied on the pore walls is given [19]:

$$\xi(t) = p_C(t)S(t) + U(t) \quad (12)$$

This equivalent pressure exerts compressive stresses on the pore walls, which leads to the shrinkage of the pore network.

3 SIMULATIONS OF THE DRYING SHRINKAGE IN CEMENT PASTE

3.1 Model parameters

The studied cement paste is composed of ordinary Portland cement (CEM I) with the mineral constitution given in Table 2. The w/c ratio is 0.4. Cement hydration is conducted in sealed conditions at 20°C (without curing). The water content decreases due to self-desiccation until the initiation of drying where the evaporation of water occurs. Four drying threshold ages were considered: t_0=0h (drying starts immediately), 6h (before setting), 12h (after setting) and 24h (during hardening).

Table 2: Mineral composition of CEM I 52.5N CE CP2 NF Villiers au Bouin.

Clinker phases	Volume fraction	Other Phases	Volume fraction
C_3S	72.2%	Gypsum	4.2%
C_2S	9.4%		
C_3A	9.4%	Calcite	1%
C_4AF	7.3%		
Arcanite	1.3%	Inert	1%
Thenardite	0.3%		

The height of the beam is 20cm (its length is assumed big enough to neglect any boundary effects on the local moisture content and so ensure 1D drying. To illustrate the effect of the

drying rate, two depths are considered: 5mm (top surface exposed to fast drying) and 2cm (slow drying). The beam is assumed to be initially fully saturated (with RH_0=100%) and its top surface exposed to an ambient humidity of 20%. Simulations are realised for four 2D specimens of the same composition in order to evaluate the repeatability.

3.2 Results and discussion

Figure 4 and 5 show the evolution of the macroscopic strain of the cement paste as a function of the hydration age, at depths 5mm and 2cm, respectively. The figures also show the effect of delayed drying on the total shrinkage strain. For the top surface at 5mm which is exposed to severe drying, the average shrinkage strain reaches high values (~4150 µm/m for t_0=0h). Cement paste starts shrinking after 1h due to the self-desiccation and the strain rate increases rapidly after 4 hours due to drying. Microcracking starts as early as 6 hours. After approximately 17hours, the rate of moisture diffusion slows down as the relative humidity approaches the critical value of 75% (Eq. 6). Another contribution of to the decrease in shrinkage rate comes from the formation of bonding between cement particles after the setting of cement paste. The relative humidity reaches a value of 65.9% after 72 hours.

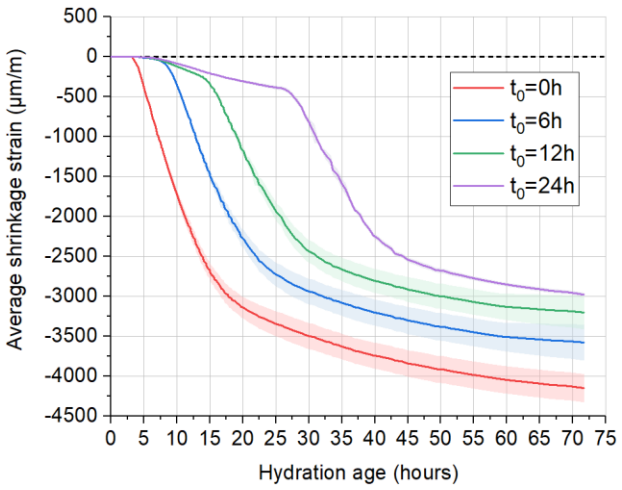

Figure 4: Total shrinkage of the cement paste as a function of the hydration age: effect of the drying threshold at depth d=5mm (shaded area = 1 S.D.)

When drying is delayed till after 6h, 12h and 24h, the shrinkage before t_0 is driven by the self-desiccation of cement paste, reaching small values of ~20µm/m, ~180µm/m and ~440µm/m, respectively, which are in agreement with experimental measurements. After t_0, cement paste undergoes severe shrinkage due to the evaporation of water. The strain reaches several magnitudes of the shrinkage due to self-desiccation. The total strain, however, decreases with increasing t_0.

The behaviour of the medium surface at drying depth d=2cm is different. For most of the computation time (<40 hours), the strain grows slowly and seems independent of t_0. This is due to the fact that intermediate layers in the cement paste beam do not start shrinking immediately, and wait until the top layers have reached low relative humidity. Therefore, the strain before 40h is the contribution of the self-desiccation shrinkage. Small deviations begin to appear after 40 hours, which suggests the beginning of drying of the 2cm–depth layer at a later hydration age.

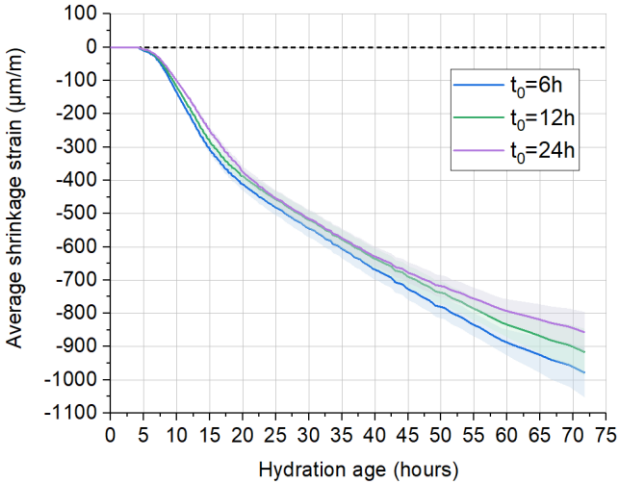

Figure 5: Total shrinkage of the cement paste as a function of the hydration age: effect of the drying threshold at depth d=2cm (shaded area = 1 S.D.).

Microcracking in cement paste can be tracked by the evolution of damage, as shown in Figure 6. For the top layer (5mm), and when drying occurs immediately (t_0=0h), the microstructure develops severe microcracking due to drying shrinkage. This is caused by the pressure build-up in the pore network, which

reaches ~59MPa at the end of the simulation. The damage map shows the beginning of the formation of a major crack in the cement paste (Figure 6, 0h). When drying occurs shortly before setting (t_0=6h), the cement paste is also severely damaged. For other drying thresholds (12h and 24h) the development of microcracks is limited as the pressure reached is not high enough to cause the fracture of the hydrate bonds formed after the setting of cement paste. These results illustrate the necessity to protect the early-age cementitious materials from drying and cracking during the first days of setting and hardening.

Compared to the top layer, the 2cm-depth layer does not show any sign of microcracks. This means that damage develops mainly at the top surface exposed to the ambient dry atmosphere, causing the scaling observed in exposed cement pastes.

The numerical results also show that the self-desiccation shrinkage does not cause the initiation of any damage. This could be explained by the relatively high w/c ratio (0.4) which is not small enough to cause severe autogenous shrinkage. Another reason is that the microstructure is not hindered. In the case of restrained deformations, the microstructure may develop microcracks that coalesce into a macrocrack that spans the whole REV.

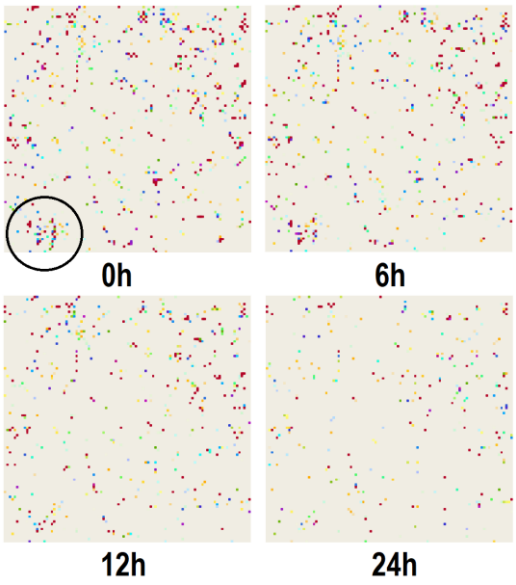

Figure 6: Microcracking in cement paste at the end of the simulation and at drying depth = 5mm, for different drying threshold ages

4 CONCLUSIONS AND PERSPECTIVES

This article presents a new methodology to simulate drying shrinkage and shrinkage-induced microcracking in cement paste. The novelty of this methodology is that the cement paste microstructure is explicitly represented and the simulations take into account the evolving nature of the material at early-ages.

The simulation results corroborate the experimental observations regarding the drying behaviour of cement paste. Notably, the drying shrinkage is several magnitudes bigger than the shrinkage caused by self-desiccation and causes more damage for the layers near the surface exposed to dry conditions. Drying causes diffuse microcracking to the cement paste even when the material is not retrained.

Further developments to the current modelling approach are needed, namely the effect of the evaporation of water from drying on the further development of the hardening microstructure. The effects of temperature and w/c ratio can also be studied in future numerical studies, as well as the influence of restrained conditions on the development of macrocracks in the cement paste.

5 REFERENCES

[1] Mounanga, P., Baroghel-Bouny, V., Loukili, A., and Khelidj, A., 2006. Autogenous deformations of cement pastes: Part I. Temperature effects at early age and micro–macro correlations *Cement and Concrete Research* 36:110–122.

[2] Baroghel-Bouny, V., Mounanga, P., Khelidj, A., Loukili, A., and Rafaï, N., 2006. Autogenous deformations of cement pastes: Part II. W/C effects, micro–macro correlations, and threshold values *Cement and Concrete Research* 36:123–136.

[3] Hansen, W., 1987. Drying Shrinkage Mechanisms in Portland Cement Paste *Journal of the American Ceramic Society* 70:323–328.

[4] Bissonnette, B., Pierre, P., and Pigeon, M., 1999. Influence of key parameters on drying shrinkage of cementitious

materials *Cement and Concrete Research* 29:1655–1662.

[5] Baănt, Z. P. and Raftshol, W. J., 1982. Effect of cracking in drying and shrinkage specimens *Cement and Concrete Research* 12:209–226.

[6] Lura, P., Jensen, O. M., and Weiss, J., 2009. Cracking in cement paste induced by autogenous shrinkage *Materials and Structures* 42:1089–1099.

[7] Havlásek, P. and Jirásek, M., Modeling Drying Shrinkage and the Creep of Concrete at the Meso-Level, in *CONCREEP 10*, 2015, :287–295.

[8] Idiart, A. E., López, C. M., and Carol, I., 2011. Modeling of drying shrinkage of concrete specimens at the meso-level *Materials and Structures* 44:415–435.

[9] Luković, M., Šavija, B., Schlangen, E., Ye, G., and van Breugel, K., 2016. A 3D Lattice Modelling Study of Drying Shrinkage Damage in Concrete Repair Systems. *Materials (Basel, Switzerland)* 9.

[10] Zhang, J., Gao, Y., Han, Y., and Wang, J., 2015. Evaluation of shrinkage induced cracking in early age concrete: From ring test to circular column *International Journal of Damage Mechanics* 26:771–797.

[11] Gao, P., Ye, G. an, Wei, J. X., and Yu, Q. J., Numerical simulation of the autogenous shrinkage of hardening Portland cement paste, in *VII European Congress on Computational Methods in Applied Sciences and Engineering*, 2016.

[12] van Breugel, K., 1995. Numerical simulation of hydration and microstructural development in hardening cement-based materials: (II) applications *Cement and Concrete Research* 25:522–530.

[13] Bullard, J. W. and Stutzman, P. E., 2006. Analysis of CCRL Portland Cement Proficiency Samples Number 151 and Number 152 Using the Virtual Cement and Concrete Reference Laboratory *Cem. Concr. Res.* 36:1548–1555.

[14] Verpaux, P., Charras, T., and Millard, A., CASTEM 2000 une approche moderne du calcul des structures, *Calcul des structures et intelligences artificielle, Pluralis*, 1988. [Online]. Available: http://www-cast3m.cea.fr.

[15] Fichant, S., Pijaudier-Cabot, G., and La Borderie, C., 1997. Continuum damage modelling: Approximation of crack induced anisotropy *Mechanics Research Communications* 24:109–114.

[16] Fichant, S., La Borderie, C., and Pijaudier-Cabot, G., 1999. Isotropic and anisotropic descriptions of damage in concrete structures *Mechanics of Cohesive-frictional Materials* 4:339–359.

[17] Rhardane, A., Élaboration d'une approche micromécanique pour modéliser l'endommagement des matériaux cimentaires sous fluage et cycles de gel-dégel, Ecole Centrale de Nantes, 2018.

[18] Bažant, Z. P. and Najjar, L. J., 1972. Nonlinear water diffusion in nonsaturated concrete *Matériaux et Constructions* 5:3–20.

[19] Hajibabaee, A., Grasley, Z., and Ley, M. T., 2016. Mechanisms of dimensional instability caused by differential drying in wet cured cement paste *Cement and Concrete Research* 79:151–158.

[20] Odler, I. and Rößler, M., 1985. Investigations on the relationship between porosity, structure and strength of hydrated Portland cement pastes. II. Effect of pore structure and of degree of hydration *Cement and Concrete Research* 15:401–410.

[21] Xi, Y., Bažant, Z. P., and Jennings, H. M., 1994. Moisture diffusion in cementitious materials - Adsorption isotherms *Advanced Cement Based Materials* 1:248–257.

[22] Brunauer, S., Skalny, J., and Bodor, E. ., 1969. Adsorption on nonporous solids *Journal of Colloid and Interface Science* 30:546–552.

[23] Coussy, O., 2005. Poromechanics of

drying and freezing cement-based materials *Revue Européenne de Génie Civil* 9:725–746.